Cluster Compounds

DOI: 10.1002/anie.200701027

A Ferromagnetic Mixed-Valent Mn Supertetrahedron: Towards Low-Temperature Magnetic Refrigeration with Molecular Clusters**

Maria Manoli, Russell D. L. Johnstone, Simon Parsons, Mark Murrie, Marco Affronte, Marco Evangelisti, and Euan K. Brechin**

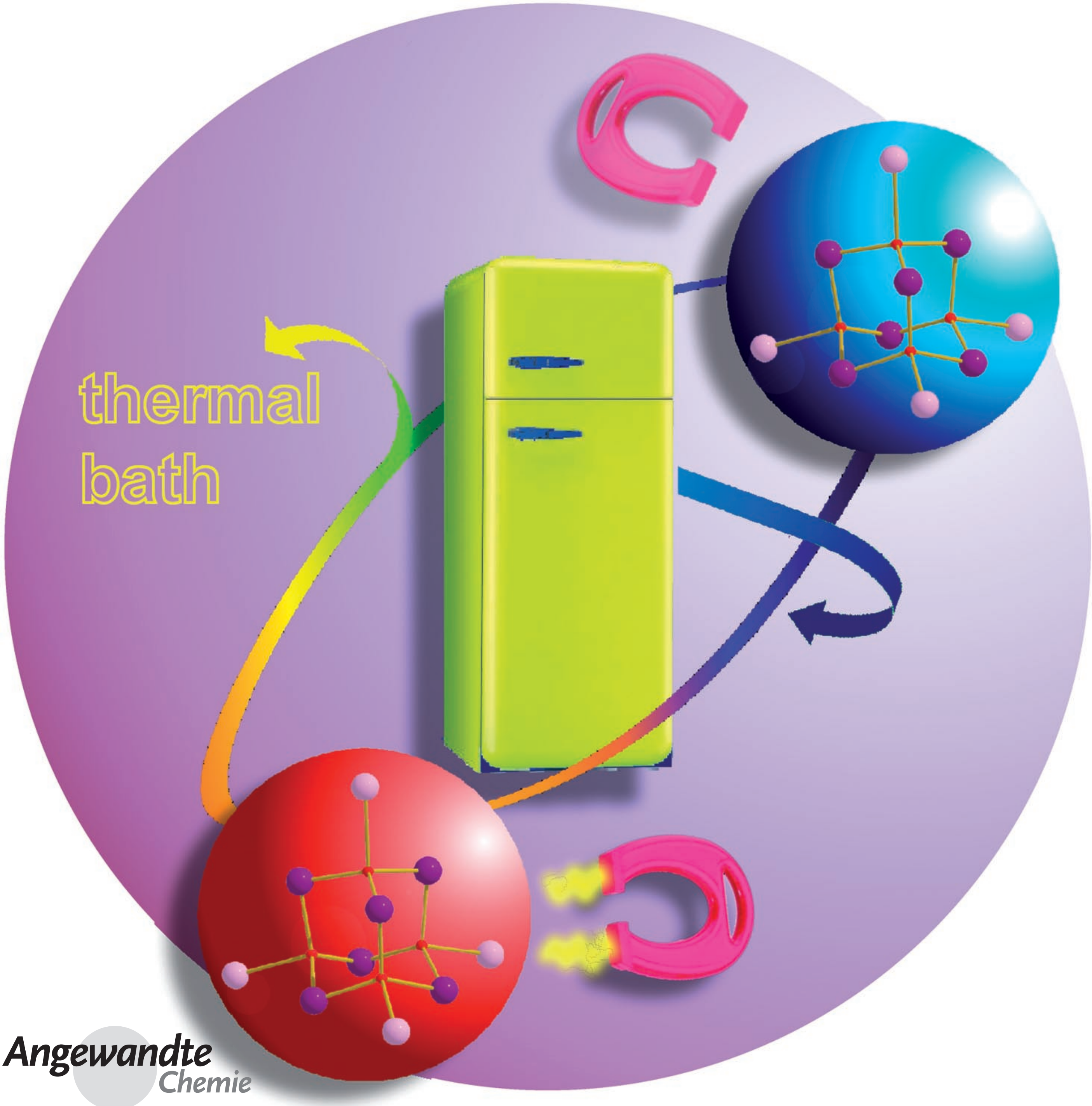

Polymetallic clusters of manganese ions come in a bewildering variety of shapes and sizes, from simple triangles,[1] cubes,[2] and butterflies,[3] to wheels,[4] discs,[5] rods,[6] truncated cubes,[7] supercubanes,[8] to the beautifully unusual and irregular.[9] The vast majority are made through self-assembly, by the simple combination of Mn^{2+} salts or $[Mn_3O(O_2CR)_6L_3]^{n+}$ triangles with flexible bridging/chelating ligands. For some time we have been investigating the coordination chemistry of the tripodal alcohols H_3thme, H_3tmp, H_4peol, and their analogues (Scheme 1) with transition-metal ions, in particular, Mn. When fully deprotonated, these ligands direct the formation of triangular $\{Mn_3\}$ units in which each oxygen atom bridges one edge of the triangle. In the presence of other bridging/chelating ligands such as carboxylates or β-diketonates, these triangles self-assemble to give a plethora of polymetallic clusters commonly based on rods, discs, tetrahedra, octahedra, and icosahedra.[10] A natural extension of these studies is the investigation of the coordination chemistry of analogous organic molecules in which one (or more) of the alcohol "arms" is replaced by an alternative functional group(s), for example, an amine group. Although each alkoxide arm has the potential to bridge up to three metal centers (and thus a maximum of seven metal centers per tripodal ligand),[11] the $-NH_2$ "arm" is likely to act solely as a monodentate/terminal capping unit, and thus the amp^{2-} ion (Scheme 1) should give rise to a number of related, yet different, structural topologies. Herein we report the synthesis and structure of a decametallic mixed-valent Mn supertetrahedron with the ligand 2-amino-2-methyl-1,3-propanediol ($ampH_2$); this cluster displays dominant ferromagnetic exchange and a spin ground state of $S=22$. Furthermore, we show that the magnetic behavior of the compound is particularly appealing in view of its possible application as an efficient low-temperature magnetic refrigerant.

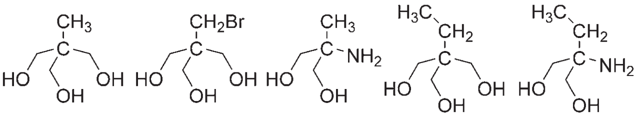

H_3thme Br-mpH_3 ampH_2 H_3tmp H_2N-H_2ep

Scheme 1. Structures of 1,1,1-tris(hydroxymethyl)ethane (H_3thme), 2-(bromomethyl)-2-(hydroxymethyl)-1,3-propanediol (Br-mpH_3), 2-amino-2-methyl-1,3-propanediol (ampH_2), 1,1,1-tris(hydroxymethyl)propane (H_3tmp), 2-amino-2-ethyl-1,3-propanediol (H_2N-H_2ep).

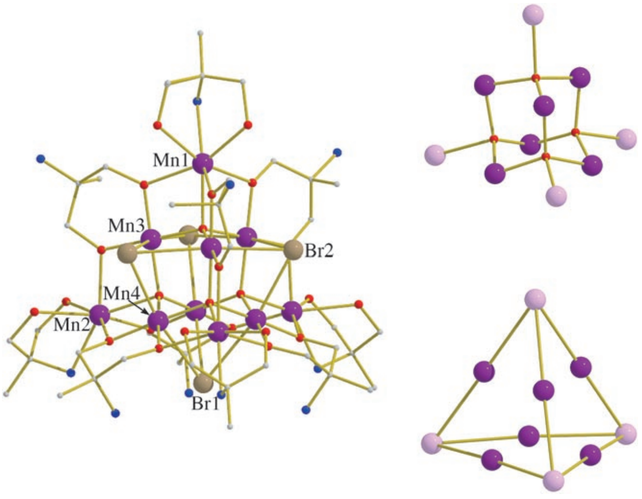

Figure 1. Left: Molecular structure of the $\{Mn_{10}\}$ cation of **1**; color code: Mn purple, O red, N blue, Br brown, C gray. Right: The central metal-oxide core of **1** (top) and its metallic skeleton (bottom); color code: Mn^{3+} purple, Mn^{2+} pink, O red.

The $\{Mn_{10}\}^{3+}$ cation (Figure 1) contains a metallic skeleton that forms a mixed-valent $\{Mn^{III}{}_6Mn^{II}{}_4\}$ supertetrahedron,[12] in which each nearest neighbor has a different oxidation state (Mn1, Mn2 = +II; Mn3, Mn4 = +III). The Mn^{2+} ions define the four apices of the tetrahedron and the Mn^{3+} ions lie along each edge. The Mn^{3+} ions themselves therefore describe a trigonal antiprism. The metal ions are connected by four central tetrahedral oxide ions to give a $\{Mn^{III}{}_6Mn^{II}{}_4O_4\}^{18+}$ core such that the supertetrahedron can be thought of as being built from four vertex-sharing $\{Mn^{III}{}_3Mn^{II}O\}^{9+}$ tetrahedra. The four bromide ions each cap one face of the tetrahedron. The tripodal ligands are of two types: six are doubly deprotonated (amp^{2-}) and bridge in a μ_3 fashion along each edge of the tetrahedron (e.g. Mn1, Mn3, and Mn2 in Figure 1), and four remain fully protonated ($ampH_2$) and chelate each Mn^{2+} vertex ion. The pendant $-NH_2$ "arms" of the amp^{2-} ligands at the triangular "base" of the cluster are H-bonded to Br^- counter ions that lie between neighboring Mn_{10} molecules. Each N atom is H-bonded to two Br^- ions at distances of approximately 3.2 Å forming head-to-head $\{Mn_{10}\}$ dimers throughout the crystal. The oxidation states of the Mn (and oxide) ions were assigned by using a combination of charge-balance and bond-length considerations, and BVS analysis. The Jahn–Teller axes of the octahedral Mn^{3+} ions are directed by the presence of the long Mn–Br bonds: thus for Mn4 their direction is defined by Br1 and Br2, and for Mn3 their direction is defined by Br2 and its symmetry equivalent atom. All the Mn^{2+} ions are seven-coordinate and bound to an

---

[*] Prof. M. Affronte, Dr. M. Evangelisti
National Research Center on "nanoStructures and bioSystems at Surfaces" (S^3)
INFM-CNR
Via G. Campi 213A, 41100 Modena (Italy)
Fax: (+39) 059-205-5651
E-mail: evangelisti.marco@unimore.it

M. Manoli, R. D. L. Johnstone, Dr. S. Parsons, Dr. E. K. Brechin
School of Chemistry
The University of Edinburgh
West Mains Road, Edinburgh, EH9 3JJ (UK)
Fax: (+44) 161-275-4598
E-mail: ebrechin@staffmail.ed.ac.uk

Dr. M. Murrie
Department of Chemistry
University of Glasgow
University Avenue, Glasgow, G12 8QQ (UK)

[**] This work was supported by the EPSRC, the Leverhulme Trust (UK), and MAGMANet (NMP3-CT-2005-515767).

$\{O_6N\}$ set of atoms. Triply bridging Br^- ions have been observed before in Mn chemistry in the complexes $[Mn_4O_3X(O_2CR)_3(dbm)_3]$ (X = halide, Hdbm = dibenzoylmethane), in which the halide sits in the corner of a distorted cubane,[13] $[Mn_6O_4Br_4(R_2dbm)_6]$, in which the halide caps the face of an octahedron,[14] and $[NMe_4]_4[Mn_{10}O_4(biphen)_4Br_{12}]$ (biphen = 2,2′-biphenoxide), in which the μ_3-halides form an $\{Mn_4Br_6\}$ adamantane-like core.[15] In each of these complexes the μ_3-Br^- ions sit on an axially elongated site with average Mn^{3+}–Br bond lengths in the range 2.79–2.84 Å, which is consistent with the values seen here (Mn–Br(av) = 2.82 Å). The charge balance of the complex is completed by the presence of the Br^- counterions and an additional proton. Significant disorder within the $\{Mn_{10}\}$ unit and in the interstitial solvent molecules[16] makes knowing its exact location difficult, but we have assumed that it is disordered over the pendant -NH_2 moieties, thus giving the complex the overall formula $[Mn_{10}O_4Br_4(amp)_6(ampH_2)_3(HampH_2)]Br_3\cdot 8$ hexane ($\mathbf{1}\cdot 8\,C_6H_{14}$).

Variable-temperature dc magnetic susceptibility data were collected on $\mathbf{1}\cdot 2.5\,C_6H_{14}$ (Figure 2) in the temperature range 300–1.8 K in an applied field of 0.1 T. The room-temperature $\chi_M T$ value of approximately 48 $cm^3\,K\,mol^{-1}$ increases upon cooling to a maximum value of approximately 224 $cm^3\,K\,mol^{-1}$ at 10 K before dropping to approximately 160 $cm^3\,K\,mol^{-1}$ at 1.8 K. The $\chi_M T$ value expected for an uncoupled $\{Mn^{III}_6Mn^{II}_4\}$ unit ($g = 2.00$) is approximately 36 $cm^3\,K\,mol^{-1}$, which is less than the measured value at 300 K. This behavior is indicative of dominant ferromagnetic exchange between the metal centers resulting in an $S = 22$ ground state—which would give a $\chi_M T$ value of approximately 253 $cm^3\,K\,mol^{-1}$. The low-temperature decrease is assigned to Zeeman effects and/or intermolecular antiferromagnetic interactions, which is consistent with the "dimeric" $\{Mn_{10}\}_2$ structure in the crystal. To determine the spin ground state for complex **1**, magnetization data were collected in the ranges 10–50 kG and 1.8–6.0 K and these are plotted as reduced magnetization ($M/N\mu_B$) versus H/T in Figure 2. The data show that saturation occurs at a value of approximately 44 and that the various isofield lines superimpose, which clearly indicates the presence of an $S = 22$ ground state with no appreciable zero-field splitting. The data were fit by a matrix-diagonalization method to afford the best fit parameters $S = 22$, $g = 2.00$, and $D = 0\,cm^{-1}$. Given the molecular symmetry (approximately T_d) of the complex, a value of, or close to, zero is expected. Thus despite the large S value, complex **1** does not behave as a single-molecule magnet, as confirmed by the lack of an out-of-phase (χ_M'') signal in ac susceptibility studies. The low-temperature in-phase $\chi'_M T$ versus T data are superimposable on the dc data.

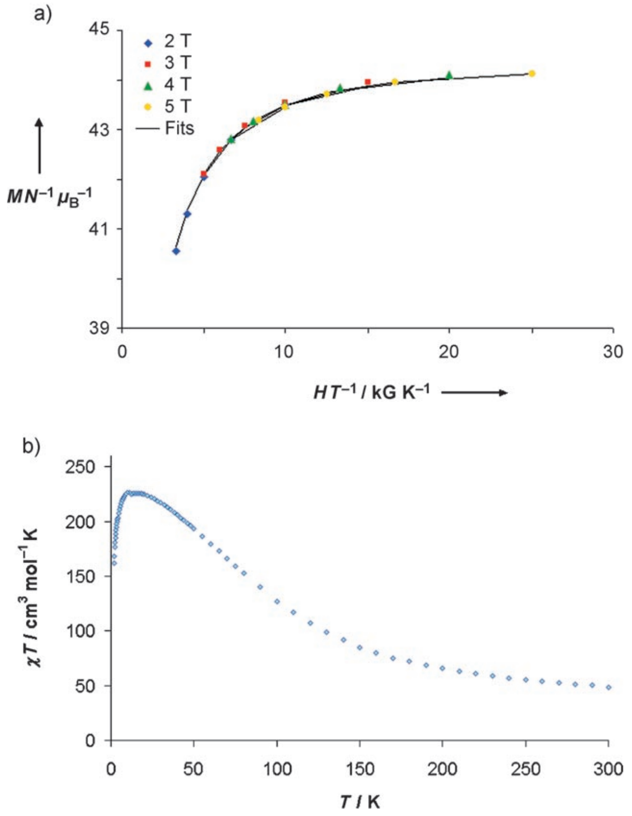

Figure 2. a) Reduced magnetization ($M/N\mu_B$) versus H/T in the ranges $T = 1.8$–6.0 K and $H = 10$–50 kG; the solid lines are a fit of the data with the parameters $S = 22$ and $D = 0\,cm^{-1}$. b) $\chi_M T$ versus T for **1** in the range $T = 2.0$–300 K.

A detailed field-dependent heat-capacity (C) investigation of **1** corroborates the analysis of the magnetization data. A relevant feature of Figure 3a is the broad specific-heat anomaly, which shifts towards higher temperatures on increasing applied field. The magnetic contribution to $C(T,H)$ for $H \geq 1$ T is due to Schottky-type Zeeman splitting of the otherwise degenerate ($D = 0\,cm^{-1}$) energy spin states. To mimic the experimental results (with powder samples), we considered molecular spins with randomly distributed orientations. The calculated results (the Schottky curves

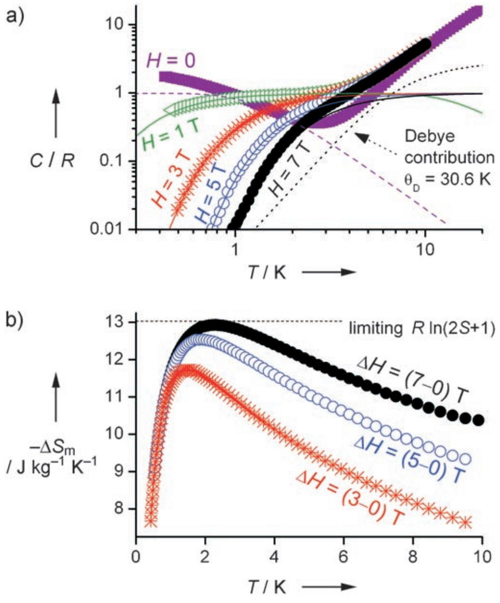

Figure 3. a) Temperature dependence of the specific heat C normalized to the gas constant R for **1** at several applied fields; the dashed and solid lines are the fits to the Schottky contributions (see text); the dotted line is the Debye fit to the lattice contribution. b) Magnetic entropy changes for **1** as obtained from the measurements of C.

depicted in Figure 3 as solid lines) perfectly reproduce the experimental magnetic curves and give $S = 22$, $g = 2$, and $D = 0\ \mathrm{cm}^{-1}$, in agreement with the $M(H)$ data. Given that $\{\mathrm{Mn}_{10}\}$ dimers are formed one would expect the appearance of an exchange field acting on each molecule which, similar to the external applied field, causes Zeeman splitting of the molecular spin ground state. Evidence for this field shows up in the experimental value of C collected at zero applied field, which follows the Schottky behavior (dashed line, Figure 3 a) calculated for $S = 22$, $g = 2$, and $D = 0\ \mathrm{cm}^{-1}$, and an exchange field of $H_{\mathrm{ex}} = 820$ G down to 1 K. For decreasing temperatures below 1 K, the intermolecular correlations become dominant, overwhelming the single-molecule behavior, and the experimental value of C continues to increase down to the minimum temperature accessible by our instrument. From the estimate of H_{ex} and given that $g\mu_{\mathrm{B}} H_{\mathrm{ex}} S = nJS^2$, we obtain the absolute value of $nJ \approx 5$ mK for the intermolecular exchange coupling.

Recent studies[17] of isotropic high-spin molecules have revealed an enhanced magnetocaloric effect (MCE), that is, the change of the magnetic entropy S_m upon a change in applied field. The interest in the MCE is both for fundamental reasons and for potential technological application, since the MCE and the associated principle of adiabatic demagnetization can be efficiently exploited for cooling applications.[17] The reason isotropic high-spin molecules are good candidates for magnetic refrigeration is twofold: 1) the higher the spin, the larger the magnetic entropy; 2) important MCEs are obtained whenever relatively small applied-field changes are sufficient to change the polarization of the magnetic molecules fully,[17] and this requires the anisotropy of the molecule to be negligible. The downside of using high-spin molecules is the presence of a large proportion of nonmagnetic constituent elements. High magnetic densities are in great demand for making devices/refrigerators of reduced size and increased efficiency. In this regard, complex **1** is a remarkable improvement because the ferromagnetic nature of the $\{\mathrm{Mn}_{10}\}$ cluster core confers a very large spin ($S = 22$) in spite of a relatively low nuclearity; that is, ferromagnetic molecules rather than antiferromagnetic ones are preferred for enhancing MCEs. Indeed, complex **1** has a spin value comparable to those of other (antiferromagnetic) molecules studied for their large MCEs,[17,18] but its molecular weight is roughly half the magnitude.

The feasibility of **1** for low-temperature magnetic refrigeration requires precise determination of the magnetic entropy change ΔS_{m} upon an applied-field change ΔH. From the experimental specific heat C data, the magnetic entropy is calculated as $S_{\mathrm{m}}(T,H) = \int C_{\mathrm{m}}/T\,\mathrm{d}T$, whereby the magnetic specific heat C_{m} is obtained from C by subtracting the lattice contribution.[19] It then becomes straightforward to obtain the entropy changes, whose temperature dependencies are depicted in Figure 3 b for several field changes. It can be seen that $-\Delta S_{\mathrm{m}}$ reaches a maximum value of $13.0\ \mathrm{J\,kg^{-1}\,K^{-1}}$ at around 2.2 K. This value is achieved for $\Delta H = (7\text{–}0)$ T and corresponds to the full change of the total magnetic entropy $R\ln(2S{+}1)$ for a spin $S = 22$ (dotted line in Figure 3 b). Notably, a $-\Delta S_{\mathrm{m}}$ value of $13.0\ \mathrm{J\,kg^{-1}\,K^{-1}}$ is among the highest values ever reported for this temperature range.[18] We finally mention that for an adiabatic demagnetization refrigerator—intended for the achievement of ultralow temperatures—the ideal initial temperature of the cooling process (by adiabatic demagnetization) is in the region of 2 K. This relatively low starting temperature, easily reached in any research laboratory by pumping liquid ^{4}He, would permit cooling to well below 0.1 K, provided that a suitable refrigerant material is selected. The above results suggest that **1** is an excellent candidate.

In conclusion, our initial investigations into the coordination chemistry of 2-amino-2-methyl-1,3-propanediol have afforded a beautiful and unusual mixed-valent decametallic Mn supertetrahedron. Complex **1** is the first characterized Mn cluster (and an extremely rare example of any transition-metal cluster) containing the amp^{2-} ligand, although we have previously reported clusters containing the closely related $\mathrm{H_2N\text{-}H_2ep}$ ligand.[20] Magnetic studies reveal that the complex possesses an extremely large spin ground state of $S = 22$ as a result of the dominant ferromagnetic exchange interactions between the metal centers. Complex **1** is thus a rare example of a molecule that displays this unusual combination. Furthermore, **1** has great potential as an efficient magnetic refrigerant in low-temperature applications.

Experimental Section

1: $\mathrm{MnBr_2{\cdot}4\,H_2O}$ (500 mg, 1.74 mmol) and ampdH$_2$ (170 mg, 1.74 mmol) were stirred in MeOH for 1 hour. The solution was then filtered and layered with hexanes. Crystals of $\mathbf{1}{\cdot}8\,\mathrm{C_6H_{14}}$ formed in 3 days in a yield of approximately 20 %. Elemental analysis (%) calcd for $\mathbf{1}{\cdot}2.5\,\mathrm{C_6H_{14}}$ ($\mathrm{C_{40}H_{100}Mn_{10}N_{10}Br_7}$): C 27.19, H 5.60, N 5.77; found: C 26.98, H 5.49, N 5.49.

Received: March 7, 2007

Keywords: cluster compounds · ferromagnetism · magnetic properties · magnetocaloric effect · manganese

---

[1] R. D. Cannon, R. P. White, *Prog. Inorg. Chem.* **1988**, *36*, 195.

[2] S. M. J. D. Aubin, M. W. Wemple, M. B. Maple, G. Christou, D. N. Hendrickson, *J. Am. Chem. Soc.* **1998**, *120*, 839.

[3] J. Yoo, E. K. Brechin, A. Yamaguchi, M. Nakano, J. C. Huffman, A. L. Maniero, L. C. Brunel, K. Awaga, H. Ishimoto, G. Christou, D. N. Hendrickson, *Inorg. Chem.* **2000**, *39*, 3615.

[4] A. T. Tasiopoulos, A. Vinslava, W. Wernsdorfer, K. A. Abboud, G. Christou, *Angew. Chem.* **2004**, *116*, 2169; *Angew. Chem. Int. Ed.* **2004**, *43*, 2117.

[5] S. Koizumi, M. Nihei, M. Nakano, H. Oshio, *Inorg. Chem.* **2005**, *44*, 1208.

[6] G. Rajaraman, M. Murugesu, E. C. Sanudo, M. Soler, W. Wernsdorfer, M. Helliwell, C. Muryn, J. Raftery, S. J. Teat, G. Christou, E. K. Brechin, *J. Am. Chem. Soc.* **2004**, *126*, 15445.

[7] R. T. W. Scott, S. Parsons, M. Murugesu, W. Wernsdorfer, G. Christou, E. K. Brechin, *Angew. Chem.* **2005**, *117*, 6698; *Angew. Chem. Int. Ed.* **2005**, *44*, 6540.

[8] a) Z. Sun, P. K. Gantzel, D. N. Hendrickson, *Inorg. Chem.* **1996**, *35*, 6640; b) A. Ferguson, K. Thomson, A. Parkin, P. Cooper, C. J. Milios, E. K. Brechin, M. Murrie, *Dalton Trans.* **2007**, 728.

[9] See, for example: a) M. Murugesu, M. Habrych, W. Wernsdorfer, K. A. Abboud, G. Christou, *J. Am. Chem. Soc.* **2004**, *126*, 4766; b) M. Soler, W. Wernsdorfer, K. Folting, M. Pink, G. Christou, *J. Am. Chem. Soc.* **2004**, *126*, 2156; c) L. F. Jones, G. Rajaraman, J.

Brockman, M. Murugesu, E. C. Sanudo, J. Raftery, S. J. Teat, W. Wernsdorfer, G. Christou, E. K. Brechin, D. Collison, *Chem. Eur. J.* **2004**, *10*, 5180.

[10] E. K. Brechin, *Chem. Commun.* **2005**, 5141.

[11] a) M. Moragues-Canovás, C. E. Talbot-Eeckalaers, L. Catala, W. Wernsdorfer, E. K. Brechin, T. Mallah, *Inorg. Chem.* **2006**, *45*, 7038; b) M. I. Khan, J. Zubieta, *Prog. Inorg. Chem.* **1995**, *43*, 1.

[12] T. C. Stamatatos, K. A. Abboud, W. Wernsdorfer, G. Christou, *Angew. Chem.* **2006**, *118*, 4240; *Angew. Chem. Int. Ed.* **2006**, *45*, 4134.

[13] S. Wang, H.-L. Tsai, E. Libby, K. Folting, W. E. Streib, D. N. Hendrickson, G. Christou, *Inorg. Chem.* **1996**, *35*, 7578.

[14] G. Aromí, M. J. Knapp, J.-P. Claude, J. C. Huffman, D. N. Hendrickson, G, Christou, *J. Am. Chem. Soc.* **1999**, *121*, 5489.

[15] D. P. Goldberg, A. Caneschi, C. D. Delfs, R. Sessoli, S. J. Lippard, *J. Am. Chem. Soc.* **1995**, *117*, 5789.

[16] Diffraction data for **1** were collected at 150 K on a Bruker Smart Apex CCD diffractometer equipped with an Oxford Cryosystems low-temperature device. The structure was solved by direct methods (SHELXS) and refined by full-matrix least squares against F^2 (CRYSTALS). CCDC-639301 contains the supplementary crystallographic data for this paper. These data can be obtained free of charge from The Cambridge Crystallographic Data Centre via www.ccdc.cam.ac.uk/data_request/cif. Crystal data for **1**$\cdot 8\,C_6H_{14}$: $C_{88}H_{212}Mn_{10}N_{10}O_{24}Br_7$, $M_r = 2599.81\ \mathrm{g\,mol^{-1}}$, $T = 150$ K, rhombohedral, space group $R\bar{3}$, $a = 15.6083(4)$, $c = 76.462(5)$ Å, $V = 16\,132.0(1)$ Å^3, $d_{\mathrm{calcd}} = 1.606\ \mathrm{g\,cm^{-3}}$, independent reflections 7364 [$R(\mathrm{int}) = 0.066$], data 7364, parameters 261, $wR2 = 0.1305$, goodness-of-fit on F^2 1.051, final $R1 = 0.0464$ for 5522 reflections with $F > 4\sigma(F)$.

[17] For a recent review, see: M. Evangelisti, F. Luis, L. J. de Jongh, M. Affronte, *J. Mater. Chem.* **2006**, *16*, 2534, and references therein.

[18] M. Evangelisti, A. Candini, A. Ghirri, M. Affronte, E. K. Brechin, E. J. L. McInnes, *Appl. Phys. Lett.* **2005**, *87*, 072504.

[19] The low-temperature and high-field experimental range turns out to be particularly relevant to determine the lattice contribution arising from acoustic low-energy phonons (Debye model). The fit provides the Debye temperature $\theta_D = 30.6$ K (dotted line in Figure 3 a).

[20] a) C. J. Milios, M Manoli, A. Mishra, L. E. Budd, F. White, S. Parsons, G. Christou, W. Wernsdorfer’E. K. Brechin, *Inorg. Chem.* **2006**, *45*, 6782; b) K. G. Alley, R. Bircher, O. Waldmann, S. T. Ochsenbein, H. U. Güdel, B. Moubaraki, K. S. Murray, F. Fernandez-Alonso, B. F. Abrahams, C. Boskovic, *Inorg. Chem.* **2006**, *45*, 8950, and references therein.